

BBABIO 43847

Stark signals associated with the reduced and oxidized states of P700 in P700-enriched particles

Stanisław Krawczyk^a and Isamu Ikegami^b

^a *Institute of Physics, Maria Curie-Skłodowska University, Lublin (Poland)* and ^b *Faculty of Pharmaceutical Sciences, Teikyo University, Sagamiko, Kanagawa (Japan)*

(Received 11 November 1992)

Key words Photosynthesis, Photosystem I, P700-enriched particle, Stark spectrum, Reaction center, CP-I, Chlorophyll-protein complex

Quadratic Stark effect was measured in the red and near infrared spectral regions for Photosystem I particles devoid of most antenna pigments, with the chlorophyll/P700 ratio of 11. Stark spectra of reduced primary electron donor exhibit a strong band at 701 nm, corresponding to a change in permanent dipole moment $\Delta\mu = 5.5 \pm 3$ D. When the primary donor is oxidized, two other bands appear at 807 nm and at 687 nm with $\Delta\mu$ equal to 5.15 D and ≈ 1.75 D, respectively. They are assigned to electronic transitions in chlorophyll cation and in neutral Chl molecule constituting the oxidized primary electron donor. In addition, two other features at ≈ 688 nm and around 670 nm were revealed, which are sensitive to the oxidation state of the primary donor. They are tentatively attributed to the primary electron acceptor A_0 and to an accessory chlorophyll *a* in the reaction center of Photosystem I. Exciton coupling and induced dipole moments are indicated as the sources of the effects observed.

Introduction

The primary electron donor in the reaction center of Photosystem I, P700, is a Chl *a* dimer possessing the main absorption band at around 700 nm [1–4]. Its molecular configuration is supposedly similar to that of the primary donor in bacterial reaction centers [5,6]. The chemical nature of the primary electron acceptor and its spectral properties were controversial until, several years ago, it was established to be a Chl *a* monomer absorbing at 690 nm [7–9].

The spectroscopic and biochemical evidence points to a structural similarity between the reaction center core on the acceptor side in PS I to that in purple bacteria [10]. In bacteria, the primary electron donor is a bacteriochlorophyll dimer assisted by two accessory BChls.

In a recent work [11], it was shown by means of Stark spectroscopy of pigment-protein complex CP-I that the Chl *a* molecules constituting the primary

electron donor, P700, are arranged sufficiently close to each other to allow for orbital overlap, which manifests in the partial charge-transfer character of electronic excitation. However, any conclusions concerning other components of the reaction center core were difficult to reach because of the presence of antenna chlorophylls (Chl/P700 ratio was about 37).

In the present work, Stark effect spectroscopy is employed to assess molecular interactions in the core of PS I reaction center. This technique is based essentially on introducing an external perturbation to electronic energy levels by the applied electric field. Using this technique to study the P700-enriched particles, we determine the change in permanent dipole moment of P700 on electronic excitation, and analyse the effect of oxidation of the primary electron donor on the neighbouring Chl molecules. The results obtained allow for the assignment of some bands in absorption and Stark spectra to the structural and functional units in PS I reaction center, including the primary electron donor, the primary acceptor and accessory chlorophyll.

Materials and Methods

Photosystem I particles were prepared from spinach chloroplasts and, after lyophilization, were extracted with diethyl ether partially saturated with water according to procedures described previously [4,12,13].

Correspondence to: S. Krawczyk, Institute of Physics, M. Curie-Skłodowska University, Radziszewskiego 10, 20-031 Lublin, Poland.
 Abbreviations: Chl, chlorophyll; BChl, bacteriochlorophyll; PS I, Photosystem I; P700, primary electron donor in Photosystem I; A_0 , primary electron acceptor in Photosystem I; DCIP, 2,6-dichlorophenylindophenol.

They were resolubilized in 10 mM phosphate buffer (pH 8.0) containing 0.4% Triton X-100. Their Chl/P700 ratio was 11.

Oxidized samples were prepared by adding potassium ferricyanide to the particle suspension to a concentration of ≈ 1 mM. After mixing, they were incubated for 2 min in an ice-bath in white light from a tungsten lamp (power density 3.5 mW/cm² for $\lambda \leq 750$ nm). Glycerol was then added up to 70% (v/v) together with the oxidant, the final concentration of which was 0.9 mM. The samples were frozen in red light from the instrument's monochromator with fully open slits.

Samples with reduced P700 were prepared by adding 5–90 mM sodium ascorbate and 0.1 mM DCIP, followed by 5 min incubation in the dark at 2°C. After adding glycerol and adjusting the concentration of the redox agents, they were kept at 2°C for different time periods, up to 4.5 h. All operations with reduced particles were performed in dim light and they were frozen in darkness.

The instrument used and the method of recording the quadratic Stark effect were as described previously [11,14].

The changes in permanent dipole moment, $\Delta\mu$, and in polarizability, $\Delta\alpha$, accompanying an electronic transition, and the values of the angle δ between $\Delta\mu$ and the electronic transition dipole moment were calculated from the formula [15,16]

$$\Delta A = \frac{(\Delta\mu)^2 F^2}{10\sqrt{2}(hc)^2} ((3 \cos^2 \delta - 1) \cos^2 \chi + 2 - \cos^2 \delta) \nu \frac{d^2(A/\nu)}{d\nu^2} + \frac{\Delta\alpha}{2\sqrt{2}hc} \frac{d(A/\nu)}{d\nu} F^2 \quad (1)$$

where F is the electric field strength (rms), ν is the wavenumber, and χ is the angle between F and the electric vector of light.

The method of estimation of the angle δ for an electronic transition represented in the Stark spectrum by a distinct negative band was based on plotting the ratio $\Delta A(\chi)/\Delta A(\chi = 90^\circ)$ vs $\cos^2 \chi$ [17]. $\Delta A(\chi)$ was determined by rotating the sample around the vertical axis in a linearly polarized light beam with horizontally oriented electric vector. The angle χ was calculated from the refraction law.

The gaussian deconvolution of absorption spectra was performed by fitting them with the sum of individual bands assumed in the form

$$A(\nu) = G \exp[-((\nu - \nu_0)/s)^2] \quad (2)$$

Results

The quadratic Stark effect was measured for samples with either reduced or oxidized primary electron

donor, P700. Each scan extended into near infrared up to 10000 cm⁻¹. Since no remarkable features were noted at wavenumbers below 11500 cm⁻¹, the spectra are displayed so as to provide insight within the relevant spectral range.

Reduced primary electron donor

Prolonged exposure of reduced samples to the measuring light beam led to slow conversion of P700 to the oxidized form. Thus, only the first few scans recorded with light of lower intensity and with no signs of changes appearing later on illumination were averaged and taken to represent the absorption and Stark spectra of reduced samples.

The absorption and Stark spectra of samples with reduced P700 are shown in Fig. 1. In the red, the Stark spectrum exhibits two negative bands at 701 nm (14265 cm⁻¹) and at 683 nm (14635 cm⁻¹). The band at 701 nm disappears on oxidation of P700. By comparison with data obtained previously for the CP-I complex [11] it can be ascribed to P700 with certainty.

The negative band at 683 nm also disappears on oxidation of P700. The position of its minimum at 683 nm indicates that it rather should not be attributed to residual P700⁺ in reduced samples, since the latter gives rise to Stark signal with minimum at 687 nm (14560 cm⁻¹, see below).

The interrupted line in Fig. 1B approximates the contribution from antenna pigments, calculated from Eqn. 1 with the first and second derivatives of the absorption spectrum. The values of $\Delta\mu = 1$ D and $\Delta\alpha = 5$ Å³ were assumed for Chl *a* in this calculation.

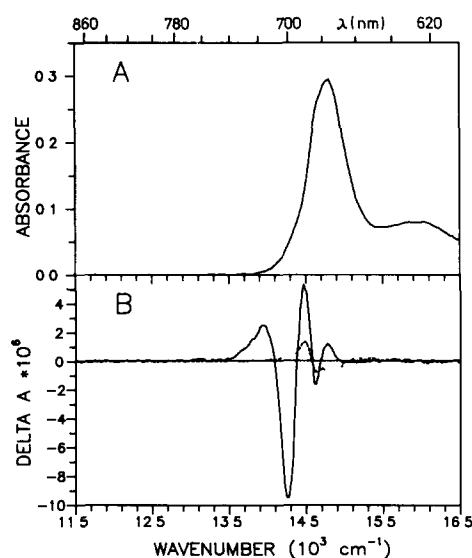


Fig. 1 Absorption and Stark spectra of P700-enriched particles in 70% glycerol in the presence of 91 mM sodium ascorbate and 0.1 mM DCIP. Temperature 130 K. (A) Absorption spectrum. (B) Stark spectrum recorded at normal incidence with the electric field strength $F = 8.78 \cdot 10^4$ V cm⁻¹ (continuous line), and the spectrum calculated from Eqn. 1 with $\Delta\mu = 1$ D, $\Delta\alpha = 5$ Å³, $\delta = 40^\circ$ (dashed line).

according to the findings for monomeric Chl *a* [14] and following the previous work on CP-I [11], and the angle δ was assumed to be equal to 40° , similar to that estimated for the weakly coupled Chl *a* in the antenna complex LHC-II [18]. As can be seen, the negative Stark band at 683 nm (14630 cm^{-1}) is very similar to the minimum at the same position that should result from antenna Chl, and thus can be ascribed partly to antenna pigments that contribute to the Stark spectrum mainly as monomeric chlorophylls. However, the strong band of P700 of presumably second-derivative shape could be expected to have a flat positive shoulder on the short-wavelength side, and thus it is possible that the minimum at 683 nm and the abnormally large positive peak at 691 nm (14470 cm^{-1}) result from the superposition of the P700 band with a first-derivative shaped (bipolar) feature centered at 687–8 nm (14540 cm^{-1}). The assumption of a hypothetical band centered at 687–8 nm leads to a quite reasonable value of its bandwidth, $s = 106\text{ cm}^{-1}$. Additionally, the overlap of a strong positive feature at 691 nm with the negative part of the P700 Stark band can at least partly account for the red-shifted position of the center of the latter band (700–701 nm) relative to the P700 absorption (697 nm) and for its higher slope on the high-wavenumber side. Further interpretation and assignment of this Stark feature is presented in Discussion.

In order to provide more direct insight into the effects observed, we calculated the difference between the observed Stark spectra and those which can be expected if all Chl molecules are noninteracting monomers. The results of subtraction are shown in Fig 2, with the dashed line representing particles with reduced P700.

At wavelength about 670 nm (14750 cm^{-1}), the signs of the Stark signals and of ΔA calculated for antenna pigments are opposite (Fig 1B). This results in the appreciable feature in the difference spectrum in Fig 2 suggesting that the Stark effect in this spectral range does not originate from weakly interacting an-

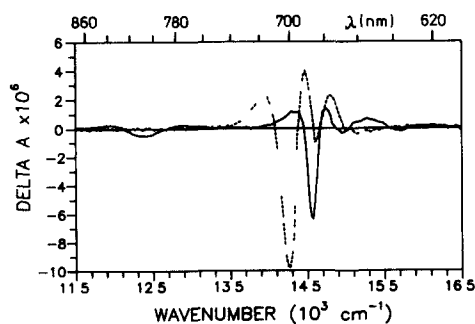


Fig 2 Difference Stark spectra for reduced (dashed line) and oxidized (continuous line) particles, resulting from subtraction of calculated Stark spectra from experimentally recorded ones shown in Figs 1B and 3B

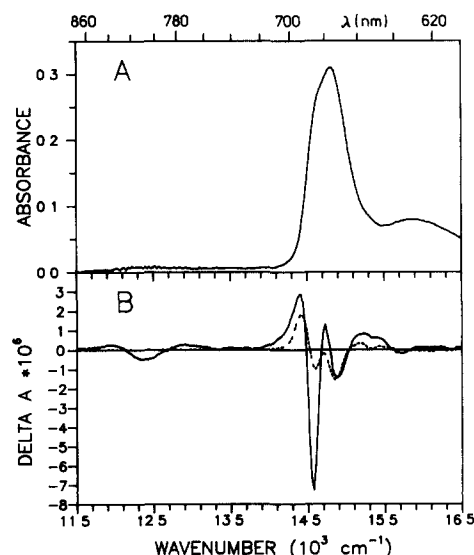


Fig 3 Absorption and Stark spectra of P700-enriched particles in 70% glycerol in the presence of 0.9 mM potassium ferricyanide. Temperature 130 K. (A) Absorption spectrum. (B) Stark spectrum recorded at normal incidence with the electric field strength $F = 8.78 \cdot 10^4\text{ V cm}^{-1}$ (continuous line), and the spectrum calculated from Eqn 1 with $\Delta\mu = 1\text{ D}$, $\Delta\alpha = 5\text{ \AA}^3$, and $\delta = 40^\circ$ (dashed line)

tenna Chl which could be considered as 'monomeric', but from a Chl with perturbed electronic states.

Thus, the analysis of the Stark spectrum of P700-enriched particles with the primary electron donor in the reduced state indicates that, besides the strong band of approximately second-derivative shape generated by the primary donor at 701 nm, two other bands at 687–8 nm and at 669 nm can be revealed, which contribute to the Stark spectrum in a more complicated manner.

Oxidized primary electron donor

The absorption and Stark spectra of oxidized samples are shown in Fig 3. They are significantly different from those obtained for reduced particles. The strong band at 701 nm disappears completely and is replaced by a narrow band at 687 nm (14560 cm^{-1}). Also, three weaker bands at 806–7 nm (12400 cm^{-1}), 671 nm (14900 cm^{-1}) and 635–6 nm (15725 cm^{-1}) appear, which were absent in the spectra of reduced particles. This indicates that the strong signals recorded with both reduced and oxidized samples originate mainly from molecules located in the core of the PS I reaction center and sensitive to the redox state of P700.

The band at 807 nm (12400 cm^{-1}) has a symmetric second-derivative shape and is related to the weak absorption band of P700^+ which appears when the reaction center of PS I is oxidized chemically or photochemically [20,21]. The appearance of respective absorption band at this wavelength is evidenced by difference spectra $A_{\text{oxd}} - A_{\text{red}}$, presented in Fig 4, for samples at normal and low temperatures. The shapes of

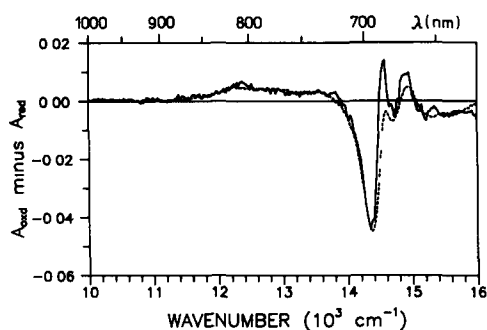


Fig 4 Difference absorption spectra (oxidized minus reduced) of P700-enriched particles at room temperature (dashed line) and at 130 K (continuous line). Room-temperature spectrum was normalized so as to facilitate comparison. It was recorded with a diluted sample in 10 mM phosphate buffer and 0.4% Triton X-100. The low-temperature spectrum is the difference of absorption spectra shown in Figs 1A and 3A.

both difference spectra are similar except for an effect of band sharpening at low temperature. Their comparison shows that the wide absorption band with the maximum around 815–820 nm ($\approx 12240 \text{ cm}^{-1}$) becomes narrower at low temperature and exhibits a quite remarkable maximum at 807 nm ($\approx 12390 \text{ cm}^{-1}$), coincident with the minimum in the Stark spectrum of oxidized particles in Fig 3B.

The appearance of a new band in Stark spectrum at 687 nm (14560 cm^{-1}) clearly corresponds to changes in absorption spectra which occur at the same wavelength on oxidation of P700. Difference spectra $A_{\text{oxd}} - A_{\text{red}}$ in Fig 4 indicate that the feature at 687 nm (14560 cm^{-1}) which remains negative at room temperature (cf. also Refs 4 and 19) becomes positive at low temperature, thus indicating the appearance of a new absorption band at this position. It corresponds to an electronic transition with dipole strength approximately equal to that for the Q_y band in monomeric Chl *a* and is ascribable to P700^+ [4].

In the shorter wavelength region, the similarity of the observed Stark spectrum and the calculated one (expected for virtually unperturbed Chls) in Fig 3B indicates that the negative band at 671 nm (14900 cm^{-1}) can be ascribed to antenna Chl. The features remaining after the subtraction of the calculated spectrum, shown in Fig 2, are too small to ascribe them a particular mechanism of the Stark effect. Nevertheless, the changes appearing in the range $14900\text{--}15300 \text{ cm}^{-1}$ on oxidation of P700 indicate that some electronic transition(s) in this spectral region are sensitive to the oxidation state of P700. Also, the small negative band at 636 nm (15725 cm^{-1}) repeatedly observed in the Stark spectra of oxidized particles (Figs 2 and 3B) has no counterpart in the Stark spectra of reduced particles, nor it can be ascribed to antenna Chl. Thus, it will be considered as originating from some Chl molecule perturbed by P700^+ . The position of this minimum at 636 nm in the Stark spectrum suggests its assignment to the Q_x transition in Chl *a*. The studies based on resonance Raman [22], absorption and Stark spectroscopy [14] have shown that the Q_x (0–0) transition in Chl *a* is spaced from Q_y (0–0) by 1150 cm^{-1} in pentacoordinated chlorophyll and overlaps with the long-wavelength slope of the Q_y (0–1) band. Since the Stark band at 636 nm appears only on oxidation of the primary donor and its spacing from the 687 nm band is about 1150 cm^{-1} , it can be related to the Q_x transition in the neutral Chl molecule, the Q_y transition of which is at 687 nm (P700^+).

Calculation of dipole moment changes

The angular dependence of the ratio $\Delta A(\chi)/\Delta A(90^\circ)$ for the relevant Stark bands is presented in Fig 5 and the values of the angle δ are quoted in the last column in Table I. The data plotted in Fig 5 represent the minima in the Stark spectra, where the

TABLE I

Summary of parameters of individual absorption bands relevant for Stark spectra

Band position cm^{-1} (nm)	Intensity ^b (absorbance units)	s , the $1/e$ width			$\Delta\mu$ (D)	δ (deg)
		$(\text{cm}^{-1})^a$	$(\text{cm}^{-1})^b$	$(\text{cm}^{-1})^c$		
14350 (697) (P700)	0.074	213–222	201	212 245 ^d	5.0–5.3	44
14560 (687) (P700^+)	0.069	127	117	135	1.75	60
12390 (807)	0.0056	–	–	365	5.15	36
14900 (671)	0.167 (red) 0.161 (oxd)	166–170	176–190	177	–	30

^a Gaussian deconvolution, Ikegami and Itoh [4].

^b Gaussian deconvolution, this work. Band intensities refer to absorption spectra shown in Figs 5 and 6.

^c This work, data obtained from the spacing of zero-crossing points in Stark spectra.

^d This bandwidth was estimated by taking the spacing between the center of Stark band and the zero-crossing point to the red.

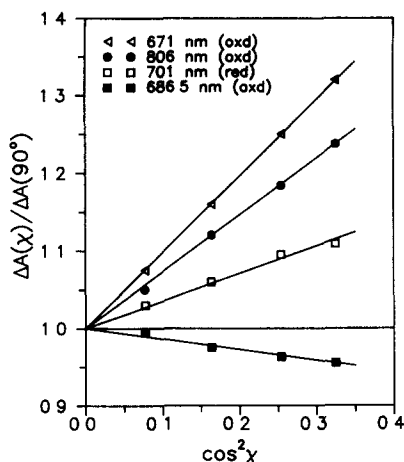


Fig 5 The angular dependence of the intensity of relevant Stark bands, measured at the wavelengths indicated χ is the angle between the vector of the applied electric field and the electric vector of light in the measuring beam

second term in Eqn 1, proportional to the first derivative, should be negligible. However, unlike Eqn 1, which is applicable to isolated molecules, calculations of band shifts and intensity changes for model systems of excitonically coupled molecules (Krawczyk, S, unpublished data) indicate that there may appear non-negligible zeroth- and first-derivative terms which depend on the angle χ , like the second-derivative term in Eqn 1. Thus, the linear relations in Fig 5 cannot solely be considered to be indicative of a particular mechanism of the Stark effect. Nevertheless, judging by the band shapes in Fig 2, two of the three most relevant Stark bands, at 807 and 687 nm, seem to fully conform to the $\Delta\mu$ -based mechanism, some level of uncertainty remains with respect to the P700 band at 701 nm due to the presence of the atypical feature on its short-wavelength side.

In the absence of precise absorption band shapes of individual electronic transitions in P700-enriched particles, the estimates of $\Delta\mu$ must rely on the approximate knowledge provided by gaussian analysis of the whole absorption spectrum. Such analysis was performed in a previous work [4]. To provide an independent set of data adequate for the P700-enriched particles used in this study, the deconvolutions were performed again with the starting values for peak positions and widths taken from the previous work [4]. Their results are given in Table I for several relevant bands and the overall fits are presented in Figs 6 and 7. The gaussian components that fit the absorption spectra of both the reduced and oxidized particles are quite analogous to those obtained with particles slightly more enriched in P700 with a Chl/P700 ratio of 10 [4].

To obtain $\Delta\mu$ for a given electronic transition from Stark data, the second derivatives in the center of respective absorption band can be calculated using

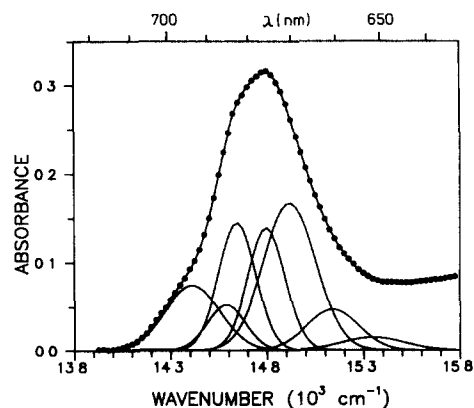


Fig 6 The gaussian components and the resulting fit of the absorption spectrum of P700-enriched particles with P700 in the reduced state. For clarity, one wide component at 15925 cm^{-1} (628 nm), with $w = 815 \text{ cm}^{-1}$, is omitted in this figure

Eqn 2 with appropriate band parameters. The bandwidths can be also determined independently of the gaussian fits, from the spacing, in cm^{-1} , of the zero-crossing points in the Stark spectra. The widths determined in this way are quoted in Table I together with those obtained from gaussian deconvolution. As can be seen, the bandwidths determined from the gaussian deconvolution agree well with the values obtained from Stark spectra under the assumption that the Stark bands are of the second-derivative shape. Also, the band positions determined by the deconvolution coincide with the minima in Stark spectra with deviations much less than the band halfwidth.

For reduced P700, it is possible to estimate the change in permanent dipole moment solely from experimental data by taking the gaussian amplitude directly from the difference spectra $A_{\text{oxd}} - A_{\text{red}}$ (Fig 4) and by assuming that the change in permanent dipole moment dominates in the electrochromism of P700. The mean experimental bandwidth ($1/e$) is 245 cm^{-1} (Table I).

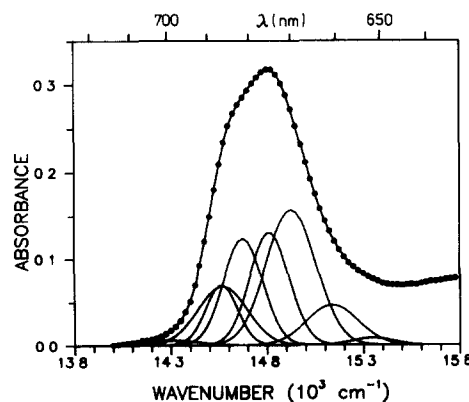


Fig 7 The gaussian components and fit of the absorption spectrum of P700-enriched particles with oxidized primary electron donor. One wide component at 15875 cm^{-1} (630 nm) with $w = 750 \text{ cm}^{-1}$ is omitted, as in Fig 6

Under these assumptions we obtain for P700 $(\Delta\mu)_{P700} = 5.0\text{--}5.3$ Debye units

If a pure first-derivative shape is assumed for the bipolar feature at 683–691 nm in the Stark spectrum of reduced particles (Fig. 1B), then a value of $\Delta\alpha$ can be calculated assuming a gaussian shape for the corresponding absorption band centered at 687–688 nm. $\Delta\alpha$ estimated from the minimum and maximum values of ΔA and from their spacing, $s \approx 120\text{ cm}^{-1}$, is between 30 and 40 \AA^3 . Since a second-derivative contribution can also be expected for this feature in Stark spectrum, this value should be considered as an upper limit for $\Delta\alpha$.

The value of $\Delta\mu$ estimated for the band at 687 nm ($P700^+$) of apparently second-derivative shape (cf. Fig. 2) with the mean bandwidth $s = 126\text{ cm}^{-1}$ (cf. Table I), is 1.75 ± 0.2 D (the error limit given here reflects the scatter in band parameters taken from gaussian deconvolutions and from Stark spectra).

The Stark and absorbance data for the electronic transition at 807 nm ($P700^+$) are the most reliable due to the lack of significant overlap of this band with other bands, as evidenced by its almost perfectly symmetrical shape in the Stark spectra. For this band, $\Delta\mu$ is 5.15 D with relative error smaller than those in previous estimates.

The estimates given above are actually the products $f\Delta\mu$, where f is the local field factor of order of 1.1–1.3 [17,23]. We quote them in this way to facilitate comparison with other Stark data. They can also bear some error inherent to the method of estimation which relies on approximating the absorption band by a pure gaussian shape.

Discussion

The interpretations of particular features in Stark spectra given in the preceding section rely upon some assumptions which, although briefly mentioned, need to be considered in more detail. The preparation used in this work contains about 11 molecules of chlorophyll per P700. Some of these are residual antenna pigments not removed by the extraction procedure, and they can potentially generate enhanced Stark features due to, e.g., strong exciton coupling like that observed for Chl *b* in antenna complex LHC-II [18]. But such features originating from antenna pigments should be rather insensitive to changes in the oxidation state of P700. Indeed, a recent study [24] points to the presence of 2–3 Chl *a* molecules absorbing at 676 nm in P700-enriched particles, which do not transfer excitation energy to P700. Therefore, the changes in Stark spectra related to P700 oxidation state must be ascribed to Chl molecules in the close neighbourhood of P700 and to P700 itself.

The value of $(\Delta\mu)_{P700} = 5\text{--}5.3$ D compares well with the previous estimate 4.7–7.7 D obtained for P700 in CP-I particles [11] and is very close to $\Delta\mu = 5.2$ D for the dimer (Chl ethanol)₂ [14]. This value was derived from the minimum in the Stark band at 701 nm under the assumption that the change in permanent dipole plays the dominant role in electrochromism of P700. However, the Stark band of P700 can contain some contributions originating from both the exciton interactions within the dimer and from its coupling with other chlorophylls in the reaction center. Simple exciton theory applied to a dimer of approximate C_2 symmetry, like the primary donors P870 or P960, predicts near cancellation of $\Delta\mu$'s of the constituent monomers in the dimer's states, and in consequence the second-derivative term near zero. However, there can be a small electric field-induced decrease of absorption intensity of dimer's P-band and a band shift to the red related to the coupling with closely lying states, which give rise to the zeroth- and first-derivative components (Krawczyk, S., unpublished data, cf. also Ref. 25). This, together with the lower value of $(\Delta\mu)_{P700}$ as compared to $(\Delta\mu)_{P870} = 6.5\text{--}7$ D and $(\Delta\mu)_{P960} = 6.5\text{--}8.2$ D [17,23], indicates that charge-transfer states may be only partly responsible for the enhanced electrochromism of P700, and the estimate for $(\Delta\mu)_{P700}$ given above should be taken as only an upper limit.

The electronic transition in $P700^+$, at 686–7 nm, is usually ascribed to the remaining Chl in the special pair present as a neutral molecule [4,19,20]. The appearance of a new absorption band at this wavelength on oxidation of P700 was inferred indirectly from the analysis of difference spectra $A_{\text{oxd}} - A_{\text{red}}$ [4,19]. The Stark spectra of both the CP-I complex [11] and of P700-enriched particles presented here clearly confirm such interpretation of difference absorption spectra. The change in permanent dipole associated with this transition, $\Delta\mu \approx 1.75$ D, can be, at least partly, ascribed to inductive effect of the Chl cation on the neutral molecule in $P700^+$. The calculations on electrochromic effects in bacterial reaction centers [26] and in free pigments [27] predict a red shift if a positive charge is placed close to ring I of the Chl or BChl molecule. Thus, the strongly red-shifted position of this absorption band would be consistent with an electrochromic effect. Additionally, an internal structure of dimeric P700 with overlapping rings I, analogous to bacterial primary electron donors [5,6], can be inferred from this red shift. The inductive effect can also explain the appearance of a weak band at 636 nm, apparently related to the Q_x transition in the same neutral Chl molecule in $P700^+$ (see Results).

Alternatively, the transition at 687 nm would be considered to result from exciton coupling in the reaction center core not necessarily involving $P700^+$, which changes significantly on oxidation of P700. However,

within the framework of exciton theory, the second-derivative contribution cannot be related to $\Delta\mu$ larger than that for monomeric Chl [18]. This circumstance points again to the assignment of the transition at 687 nm rather to $P700^+$.

The electronic transition at 807 nm ($12\,390\text{ cm}^{-1}$), related to symmetric Stark band of $P700^+$ at the same wavelength, clearly corresponds to the weak absorption band of cation radical of Chl *a* at 813 nm (at 77 K) [28] or at 824–840 nm at room temperature [21,29,30]. The radical cation of the dimer (Chl methanol)₂ possesses an absorption band at 956 nm at 77 K [28]. Thus, the band at 807 nm corresponds rather to the electronic excitation of an essentially monomeric Chl cation constituting a half of $P700^+$. It is difficult to conclude whether its $\Delta\mu = 5.15\text{ D}$ reflects a permanent dipole change of Chl^+ (which is not known), or should be related to a weak charge transfer between the halves of $P700^+$ (see below). In bacterial primary donors, analogous transitions are found at 1250 nm for $P870^+$ [31] and at 1300 nm for $P960^+$ [32], i.e., at lower energy than the near-infrared band in BChl *a* cation radical which is at $\approx 900\text{ nm}$ [33].

The above interpretation of the experimental results refers to a model of $P700$ in which the two Chl molecules are energetically inequivalent to a degree that allows the electronic states in $P700^+$ to be considered approximately as localized on either one or the other molecule, and in which the molecules are held by their protein environment so that the orbital overlap is kept sufficiently low for $(\Delta\mu)_{P700}$ to not exceed $\approx 5\text{ D}$.

In a recent study [34], it has been shown that the orbital overlap and subunit interaction in oxidized bacterial primary donors $P870^+$ and $P960^+$ result in a bonding–antibonding combination of molecular orbitals in the ground state, analogous to that in sandwich porphyrin dimers [35,36]. The resulting splitting of states leads to the appearance of an electronic absorption band in the mid-infrared region at energy as low as 2700 cm^{-1} . The intensity of this band is predicted to increase with the increase of electron delocalization over the two BChls. On this basis, a high degree of electron localization on one of the two BChls has been inferred, which results from $\approx 2000\text{ cm}^{-1}$ difference between energies of the basis states L^+M and LM^+ [34]. Such energetic asymmetry (and possibly a somewhat smaller orbital overlap) is indeed a prerequisite for spectroscopic distinction of states corresponding to separate excitations of the neutral molecule and the radical cation in $P700^+$. It should be mentioned that the description in terms of closely localized states is only approximate, and in fact there must always be some degree of electron delocalization in a system of closely spaced molecules. Spectroscopic investigations in the mid-infrared region analogous to that just mentioned [34] would be extremely helpful in establishing

the degree of delocalization of the electronic states in $P700^+$.

The positive feature observed at 691 nm ($14\,470\text{ cm}^{-1}$) in Stark spectra corresponding to reduced $P700$ (Figs 1 and 2) appears in a similar proportion to $P700$ minimum at 701 nm also in the Stark spectra of CP-I complex which contains more antenna pigments (Chl/ $P700$ ratio about 40) [11]. This band cannot be attributed to the higher-energy exciton component of $P700$, since it would be difficult to reconcile the small splitting in the $P700$ band with the strong exciton interaction between the Chl subunits. If not reflecting an intrinsic property of $P700$, the positive Stark band at 691 nm and its negative counterpart at 683 nm must be attributed to an electronic transition resulting from exciton coupling of $P700$ with a Chl molecule always present in the core of the PS I reaction center at a constant proportion to $P700$. This conclusion is in agreement with CD spectra of $P700$ -enriched particles, which show a symmetric bipolar feature centered around 688 nm (at room temperature) [37]. At present, only one candidate for such a molecule positioned close to $P700$ and absorbing at around 685–690 nm can be indicated, this is the primary electron acceptor A_0 . Thus, we propose the following interpretation of the effects observed (for simplicity, we describe the situation in terms of localized transitions while in fact they are all delocalized to some degree). Due to the coupling of A_0 with $P700$ through transition–dipole interaction, the electronic transition localized mainly on A_0 is accompanied by a significant increase in polarizability, and this adds a first-derivative shape to the respective Stark band. When the primary electron donor becomes oxidized, the exciton coupling of A_0 changes and its absorption band slightly shifts to longer wavelengths, this is the bandshift effect at 688 nm ($\approx 14\text{ nm}$ to the red) noted in photoselection experiments [19]. In this state, the Stark effect related to A_0 is weaker and probably characteristic for Chl *a* monomer.

The exciton effects in the Stark spectrum, resulting from coupling of electronic transition moments in A_0 , $P700$, and possibly other chlorophylls, are analogous to somewhat weaker effects of this kind in bacterial reaction centers [25]. They found experimental evidence in Stark spectra of bacterial antenna complexes. Also, we have found a significant contribution from the polarizability change (first-derivative term) in the Stark effect of Chl *b* in plant light-harvesting complex LHC-II [18]. However, no significant deviations from the $\Delta\mu$ -based mechanism of the Stark effect were observed for primary donors or acceptors in bacterial reaction centers, where only minor discrepancies were noted [17]. This difference between bacterial and PS I reaction centers gains a clear physical basis if we consider the differences in excitation energy of individual units in both reaction centers. In bacterial reaction centers, the ex-

cited states of primary donors P870 and P960 are lower in energy than the other electronic states by $\approx 1000 \text{ cm}^{-1}$ and $\geq 1500 \text{ cm}^{-1}$, respectively. These large differences make the electric field-induced mixing of states very weak and the first- and zeroth-derivative terms resulting from such mixing can be very small. In the PS I reaction center, the spectra are more congested and the energy difference between excited states of, e.g., A_0 and P700 is 200 cm^{-1} or less, this is the factor leading to the substantial enhancement of the untypical Stark feature centered around 687–8 nm.

The changes in Stark spectra at about 670 nm (Figs 2 and 3) cannot be clearly interpreted. The difference Stark spectra in Fig. 2 can be viewed as indicating a red shift of some absorption band at about 665–670 nm, taking place on oxidation of P700. Such a band-shift effect can account for the bipolar feature around 665–7 nm (15000 cm^{-1}) in absorption difference spectra $A_{\text{oxd}} - A_{\text{red}}$ in Fig. 4. Also, there are several experimental findings in the literature which point to the presence of an electronic transition at about 670 nm which is sensitive to the oxidation state of the primary donor. These are the observations of the bleaching of a chlorophyllous absorption band at 670 nm in PS I particles under strongly reducing conditions, originally ascribed to photoaccumulation of reduced secondary electron acceptor A_1 [39] and then of reduced A_0 [40]. Also, picosecond absorption difference spectra were found to exhibit a clear shoulder at 670 nm, in addition to the bleached band of A_0 at 690 nm, when PS I particles were excited at 710 nm [7]. Excitation at 532 nm did not produce such a shoulder [8]. Its occurrence was explained by possible side reactions of antenna pigments when excited with 710 nm light. This explanation seems to be in contradiction to what could be expected for excitation wavelengths used, nevertheless, the appearance of a bleach of picosecond duration at 670 nm remains a fact. Thus, we see it justified to relate the variable features in Stark spectra at $\approx 670 \text{ nm}$ with an accessory Chl analogous to the accessory BChls in bacterial reaction centers [5,6]. Although only hypothetical, such an assignment would be consistent with the observation that Chl *a* absorbing at 670 nm is among a few spectral forms in the PS I reaction center capable to efficiently transfer the excitation energy to P700 [24]. In the PS II reaction center, accessory chlorophylls have been revealed as the species absorbing at approximately the same wavelength [41–43].

Acknowledgement

This work was supported by the Polish Committee for Scientific Research

References

- Katz, J.J., Shipman, L.L. and Norris, J.R. (1979) CIBA Found Symp. 61, 1–34.
- Lagoutte, B. and Mathis, P. (1989) Photochem. Photobiol. 49, 833–844.
- Moenne-Loccoz, P., Robert, B., Ikegami, I. and Lutz, M. (1990) Biochemistry 29, 4740–4746.
- Ikegami, I. and Itoh, S. (1988) Biochim. Biophys. Acta 934, 39–46.
- Deisenhofer, J., Epp, O., Miki, K., Huber, R. and Michel, H. (1984) J. Mol. Biol. 180, 385–398.
- Feher, G., Allen, J.P., Okamura, M.Y. and Rees, D.C. (1989) Nature 339, 111–116.
- Shuvalov, V.A., Nuijs, A.M., van Gorkom, H.J., Smit, H.W.J. and Duysens, L.N.M. (1986) Biochim. Biophys. Acta 850, 319–323.
- Nuijs, A.M., Shuvalov, V.A., Van Gorkom, H.J., Plyter, J.J. and Duysens, L.N.M. (1986) Biochim. Biophys. Acta 850, 310–318.
- Mathis, P., Ikegami, I. and Setif, P. (1988) Photosynth. Res. 16, 203–210.
- Nitschke, W. and Rutherford, A.W. (1991) Trends Biochem. Sci. 16, 241–245.
- Krawczyk, S. and Maksymiec, W. (1991) FEBS Lett. 286, 110–112.
- Ikegami, I. and Katoh, S. (1975) Biochim. Biophys. Acta 376, 588–592.
- Ikegami, I. and Ke, B. (1984) Biochim. Biophys. Acta 764, 70–79.
- Krawczyk, S. (1991) Biochim. Biophys. Acta 1056, 64–70.
- Reich, R. and Schmidt, S. (1972) Ber. Bunsenges. Physik. Chem. 76, 589–598.
- Liptay, W. (1965) Z. Naturforsch. 20A, 272–289.
- Losche, M., Feher, G. and Okamura, M. (1987) Proc. Natl. Acad. Sci. USA 84, 7537–7541.
- Krawczyk, S., Krupa, Z. and Maksymiec, W. (1993) Biochim. Biophys. Acta 1143, 273–281.
- Schaffernicht, H. and Junge, W. (1981) Photochem. Photobiol. 34, 223–232.
- Inoue, Y., Ogawa, T. and Shibata, K. (1973) Biochim. Biophys. Acta 305, 483–487.
- Mathis, P. and Setif, P. (1981) Isr. J. Chem. 21, 316–320.
- Krawczyk, S. (1989) Biochim. Biophys. Acta 976, 140–149.
- Lockhart, D.J. and Boxer, S.G. (1988) Proc. Natl. Acad. Sci. USA 85, 107–111.
- Iwaki, M., Mimuro, M. and Itoh, S. (1992) Biochim. Biophys. Acta 1100, 278–284.
- Scherer, P.O.J. and Fischer, S.F. (1986) Chem. Phys. Lett. 131, 153–159.
- Hanson, L.K., Fajer, J., Thompson, M.A. and Zerner, M.C. (1987) J. Amer. Chem. Soc. 109, 4728–4730.
- Eccles, J. and Honig, B. (1983) Proc. Natl. Acad. Sci. USA 80, 4959–4962.
- Hoshino, M., Ikehara, K., Imamura, M., Seki, H. and Hama, Y. (1981) Photochem. Photobiol. 34, 75–81.
- Davis, M.S., Forman, A. and Fajer, J. (1979) Proc. Natl. Acad. Sci. USA 76, 4170–4174.
- Heald, R.L., Callahan, P.M. and Cotton, T.M. (1988) J. Phys. Chem. 92, 4820–4824.
- Dutton, P.L., Kaufmann, K.J., Chance, B. and Rentzepis, P.M. (1975) FEBS Lett. 60, 275–280.
- Davis, M.S., Forman, A., Hanson, L.K., Thornber, J.P. and Fajer, J. (1979) J. Phys. Chem. 83, 3325–3332.
- Fajer, J., Borg, D.C., Forman, A., Felton, R.H., Dolphin, D. and Vegh, L. (1974) Proc. Natl. Acad. Sci. USA 71, 994–998.
- Breton, J., Nabadryk, E. and Parson, W.W. (1992) Biochemistry 31, 7503–7510.

- 35 Duchowski, J K Bocian, D F (1990) *J Am Chem Soc* 112, 3312–3318
- 36 Perng, J -H, Duchowski, J K and Bocian, D F (1991) *J Phys Chem* 95, 1319–1323
- 37 Ikegami I and Itoh, S (1986) *Biochim Biophys Acta* 851, 75–85
- 38 Gottfried, D S, Stocker, J W and Boxer, S G (1991) *Biochim Biophys Acta* 1059, 63–75
- 39 Swarthoff, T, Gast, P Ames, J and Buisman H P (1982) *FEBS Lett* 146, 129–132
- 40 Mansfield, R W and Evans, M C W (1985) *FEBS Lett* 190 237–241
- 41 Telfer, A, De Las Rivas, J and Barber, J (1991) *Biochim Biophys Acta* 1060, 106–114
- 42 Telfer, A He, W -Z and Barber J (1990) *Biochim Biophys Acta* 1017, 143–151
- 43 Otte, S C M, Van der Vos, R and Van Gorkom, H J (1992) *J Photochem Photobiol Biol* 15, 5–14